Supporting information

Nickel Metal-Organic Framework Nanosheets as Novel Binder-Free Cathode for Advanced Fibrous Aqueous Rechargeable Ni-Zn Battery

Chaowei Li[a,d+], Qichong Zhang[c+], Taotao Li[b], Bing He[d], Ping Man[d], Zezhou Zhu[d], Zhenyu Zhou[d], Lei Wei[c], Kai Zhang[b], Guo Hong,[e*] Yagang Yao[b*]

[a] Henan Key Laboratory of New Optoelectronic Functional Materials, College of Chemistry and Chemical Engineering, Anyang Normal University, 436 Xian'ge Road, Anyang 455000, P. R. China

[b] National Laboratory of Solid State Microstructures, College of Engineering and Applied Sciences, Jiangsu Key Laboratory of Artificial Functional Materials, and Collaborative Innovation Center of Advanced Microstructures, Nanjing University, Nanjing 210093, China

[c] School of Electrical and Electronic Engineering, Nanyang Technological University, 50 Nanyang Avenue, 639798, Singapore

[d] Division of Advanced Nanomaterials, Key Laboratory of Nanodevices and Applications, Joint Key Laboratory of Functional Nanomaterials and Devices, CAS Center for Excellence in Nanoscience, Suzhou Institute of Nano-tech and Nano-bionics, Chinese Academy of Sciences, Suzhou 215123, China

[e] Institute of Applied Physics and Materials Engineering, University of Macau. Department of Physics and Chemistry, Faculty of Science and Technology, University of Macau. Avenida da Universidade, Taipa, Macau SAR 999078, P. R. China.

*Corresponding Author's Email: ygyao2018@nju.edu.cn; ghong@um.edu.mo

Materials

Nickel acetate tetrahydrate [$Ni(CH_3COO)_2 \cdot 4H_2O$], Zinc sulfate heptahydrate ($ZnSO_4 \cdot 7H_2O$), 2,6-naphthalenedicarboxylate potassium, Zinc oxide (ZnO), and Potassium hydroxide (KOH) were supplied by Sinopharm Chemical Reagent, China. The pristine carbon nanotube fiber (p-CNTF) are supplied by Suzhou Creative Nano Technology Co. LTD. All the chemical reagents are obtained from commercial sources and without any further purification.

Experimental section

Synthesis of Ni-MOF/CNTF electrode:

Firstly, a piece of pristine CNTF (p-CNTF, 4 cm×Φ0.015 cm) was treated at oxygen plasma generator (50 W) for 3 min to acquire oxygen plasma treated CNTF (CNTF). Then, the CNTF was fixed by polyethylene terephthalate (PET) holder and immersed into a 50 ml teflon vial containing 40 ml of DI-water and 400 mg of $Ni(CH_3COO)_2 \cdot 4H_2O$. Next, 400 mg of organic ligand 2,6-naphthalenedicarboxylate potassium was added into the above solution, and the vial was sealed for reaction at 80 ^oC for 20 h. After cooling down to room temperature, the Ni-MOF/CNTF samples were taken out, ultrasonicated for 1 min, then washed several times by DI-water and last dried in vacuum oven at 80 ^oC for 2h. The Ni-MOF powders were also cllected in order to investigate the effect of thermal treatment on the property of Ni-MOF.

Synthesis of Ni-MOF/CNTF-350 ^oC and Ni-MOF-350 ^oC:

The thermal treatment of Ni-MOF/CNTF samples and Ni-MOF powders was proceeded in a horizontal electrical resistance heated furnace (Hefei Kejing Materials Technology Co., LTD, GSL-1700X) with a temperature zone of about 30 cm, consisting of an quartz tube 60 cm in length and 25

mm in diameter. The Ni-MOF/CNTF samples and Ni-MOF powders were placed in the tube furnace and annealed in air at 350 °C for 90 min with the heating rate of 1 °C min^{-1}, and then cooled naturally to room temperature for obtaining the Ni-MOF/CNTF-350 ^{o}C and Ni-MOF-350 ^{o}C.

Fabrication and assembly of the fiber-shape aqueous rechargeable (FAR) Ni-Zn battery:

Firstly, The Zn wire (Φ=0.03 cm) electrode connected with CNTF was inserted into the heat-shrinlable pipe from one end of the tube and sealed by a Gluegun (ARZ-RJQ). Subsequently, the four Ni-MOF/CNTF twisted into a fiber electrode covered by Al_2O_3 separator was inserted into the heat-shrinlable tube from another end of the pipe. Then, the ZnO saturated 2M KOH solution was injected into the unshaped battery though the opened end. Last, the opened end of unshaped battery was sealed by the Gluegun forming a mechanically robust FAR Ni-Zn battery.

Characterizations

Morphologies of the samples are characterized by a scanning electron microscope (SEM) (Hitachi S-4800, 5 kV) and the microstructure and high-resolution transmission electron microscope (TEM) images are obtained via a FEI Tecnai G220 high-resolution transmission electron microscope at an acceleration voltage of 200 kV. A Rigaku D/MAX2500 V X-ray diffraction (XRD) with Cu Kα radiation (λ=1.5418 Å) is applied to gain the X-ray diffraction patterns of samples. X-ray photoelectron spectroscopy (XPS) on an ESCALab MKII X-ray photoelectron spectrometer with non-monochromatized Mg Kα X-rays as the excitation source is utilized to analyze the chemical element composition and oxidation states of samples. The surface area of the electrode was determined by the Brunauer-Emmett-Teller (BET) method, based on the amount of N_2 adsorbed at pressures $0.05 < P/P_0 < 0.3$ (ASAP 2020, Micromeritics, USA). The quarter mass of Ni-MOF on

CNTF electrode (0.51 mg/cm^2) was obtained by electronic balance (METTLER TOLEDO XPU, 0.1 μg). The contact angle measurements of the oxygen plasma treated CNTF (CNTF) and CNTF were performed by a Video-Optical contact Angle Instrument (Data Physics Instruments, OCA15EC) at water mode. The thermal decomposition behavior of Ni-MOF powder in air was studied by thermogravimetric analysis (TGA; Netzsch Instruments model 209 F1 Libra). The temperature was increased from 25 to 600 °C (the ramping rate was 10 °C/min).

The electrochemical measurements are performed using an electrochemical workstation (CHI 760E, Chenhua). Electrochemical properties of the electrodes are measured by a three-electrode system in ZnO saturated 2M KOH aqueous electrolyte. The materials, the Pt wire and Ag/AgCl are used as the working, counter and reference electrodes, respectively. The electrochemical impedance spectroscopy (EIS) measurements are carried out at frequencies from 10^{-2} Hz to 10^5 Hz. The performances of the Ni-Zn devices are tested in a two-electrode system.

The current density and specific capacity were defined by total area of electrode and battery which were calculated by the equation (1)

$$A = \pi \times D \times L \qquad (1)$$

Where the π is 3.14, D is the diameter of electrode and fibrous battery, and the L is the length of electrode and battery. The capacity (C), energy density (E), and powder density (P) were calculated according to the following equations:

$$C = I \times \Delta t / A \qquad (2)$$

$$E = C \times V_p \qquad (3)$$

$$P = E / \Delta t \qquad (4)$$

Where A are the total area of the as-assembled Ni-Zn battery, respectively. I, Δt and V_p represent the discharge current, discharge time, and voltage platform, respectively. We added them in revised Supporting Information and marked in blue colour.

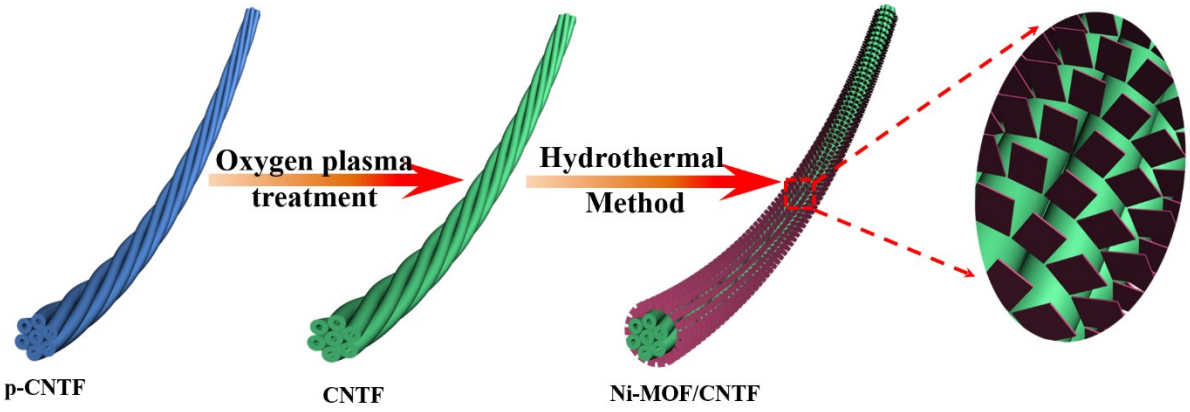

Figure S1 The schematic diagram of preparation process of Ni-MOF/CNTF.

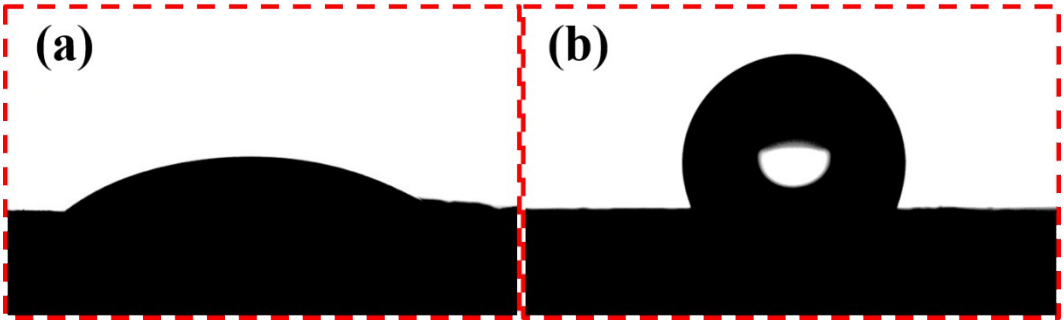

Figure S2 (a) Contact angle measurements of the CNTF (32°) and (b) Contact angle measurements of the CNTF (136°).

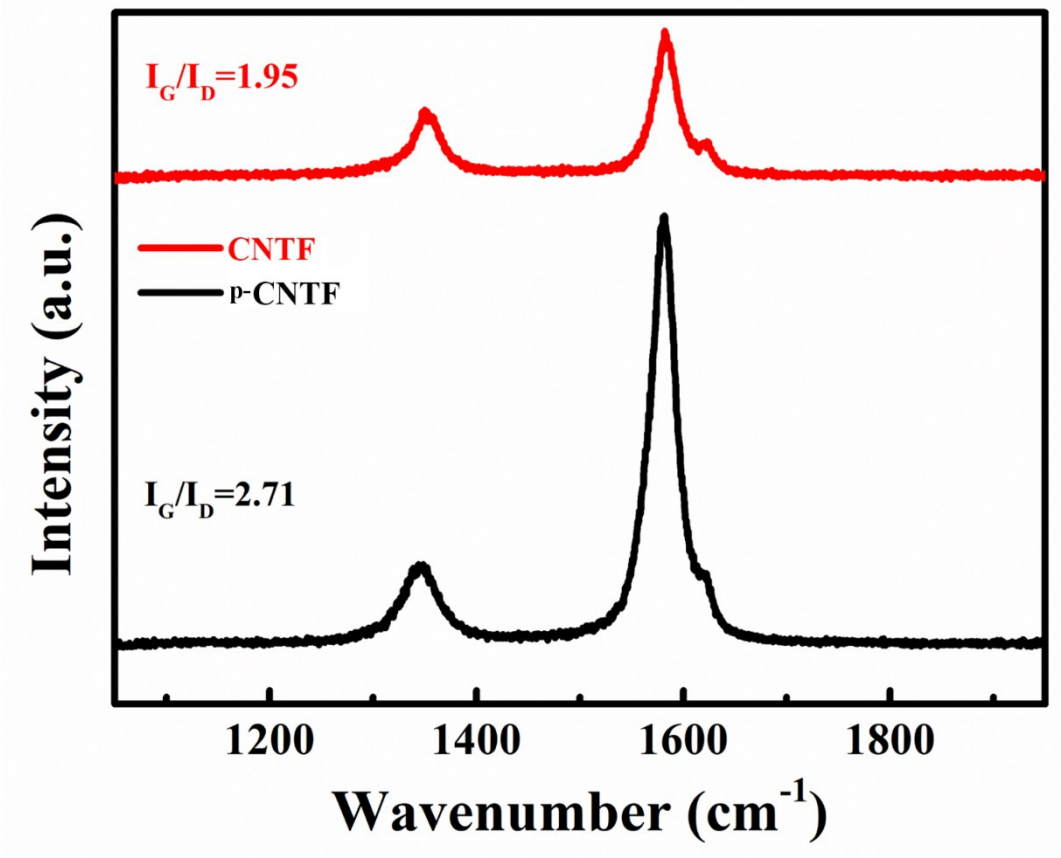

Figure S3 Raman spectra of the p-CNTF and CNTF.

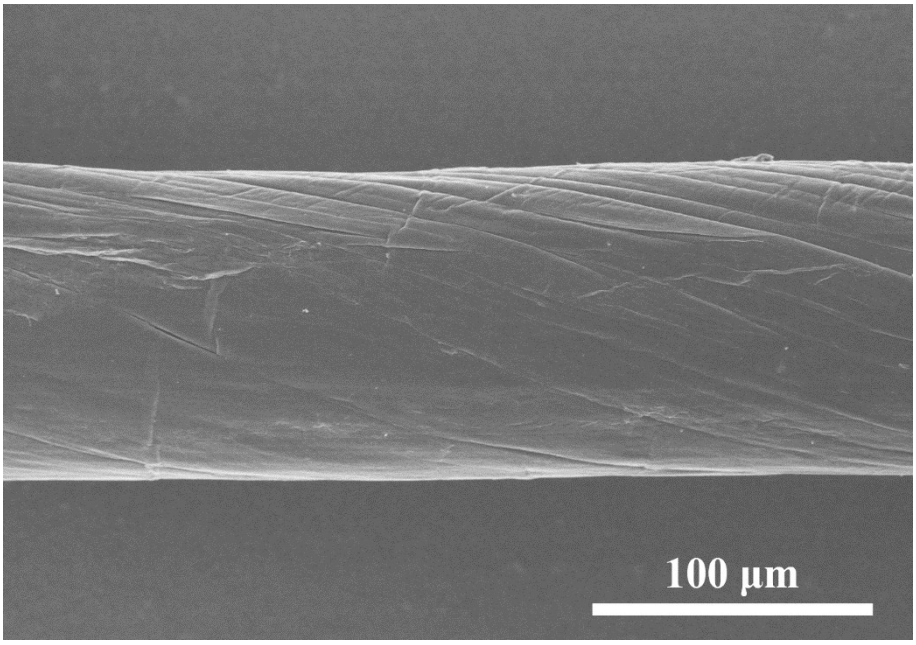

Figure S4 The SEM image of CNTF.

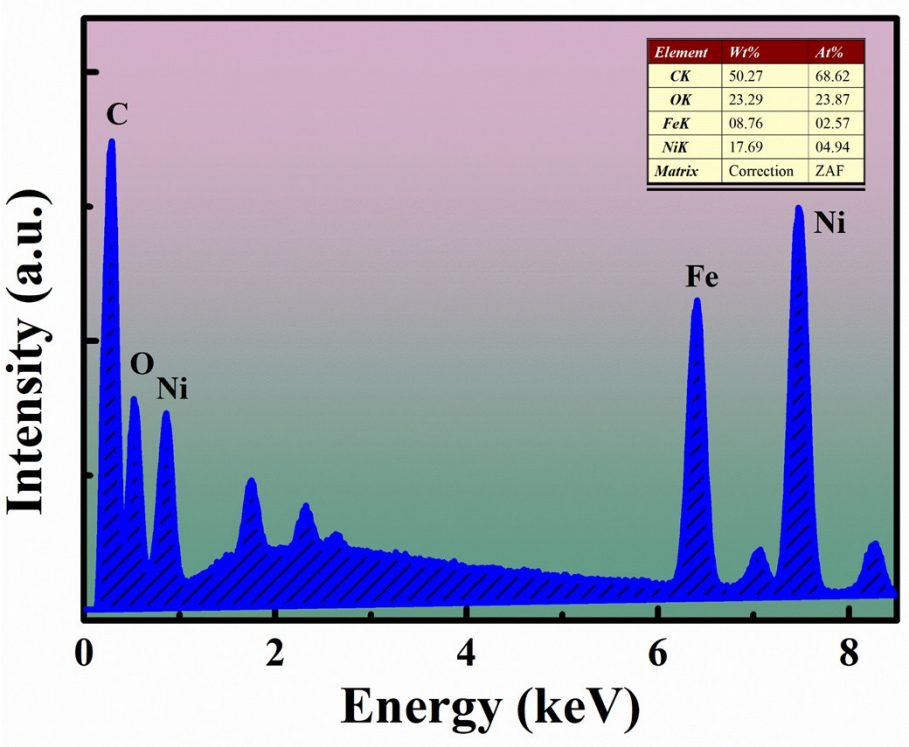

Figure S5 The energy dispersive X-ray spectrometry (EDS) of Ni-MOF/CNTF.

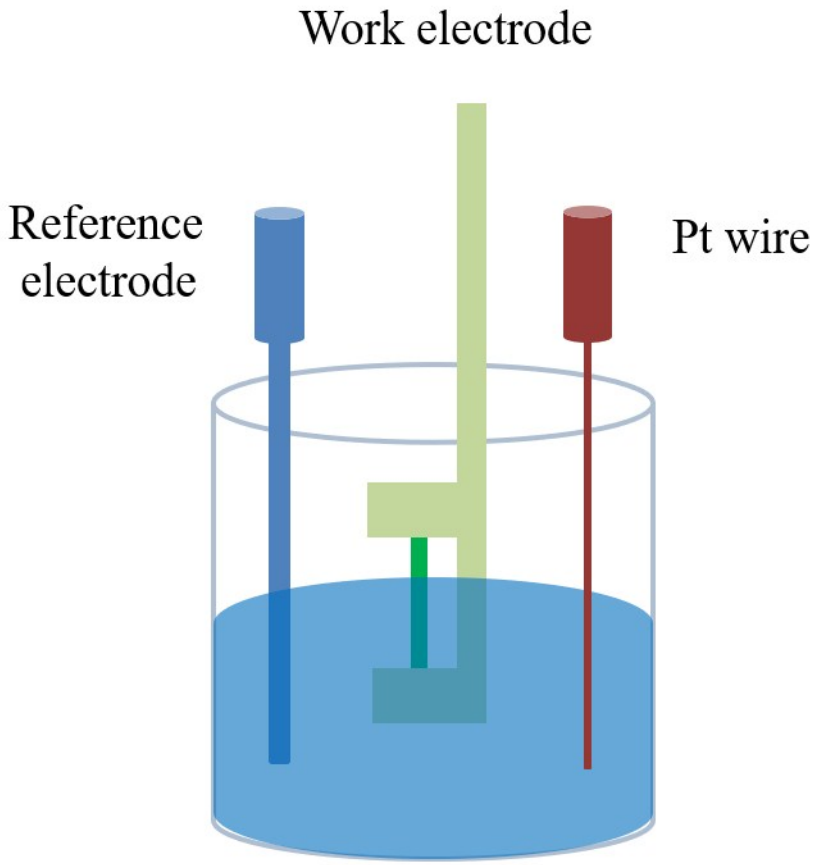

Figure S6 The schematic diagram of three-electrode test system.

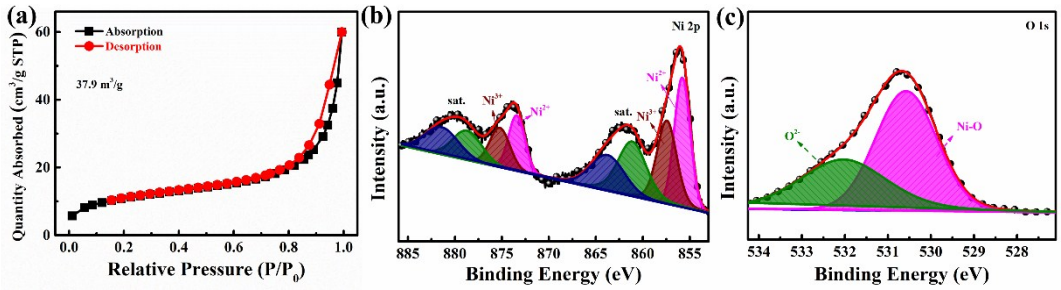

Figure S7 (a) The N_2 absorption-desorption isotherm of Ni-MOF-350 ^oC; (d) Core level Ni 2p XPS spectrum of Ni-MOF-350 ^oC; (e) Core level O 1s XPS spectrum of Ni-MOF-350 ^oC.

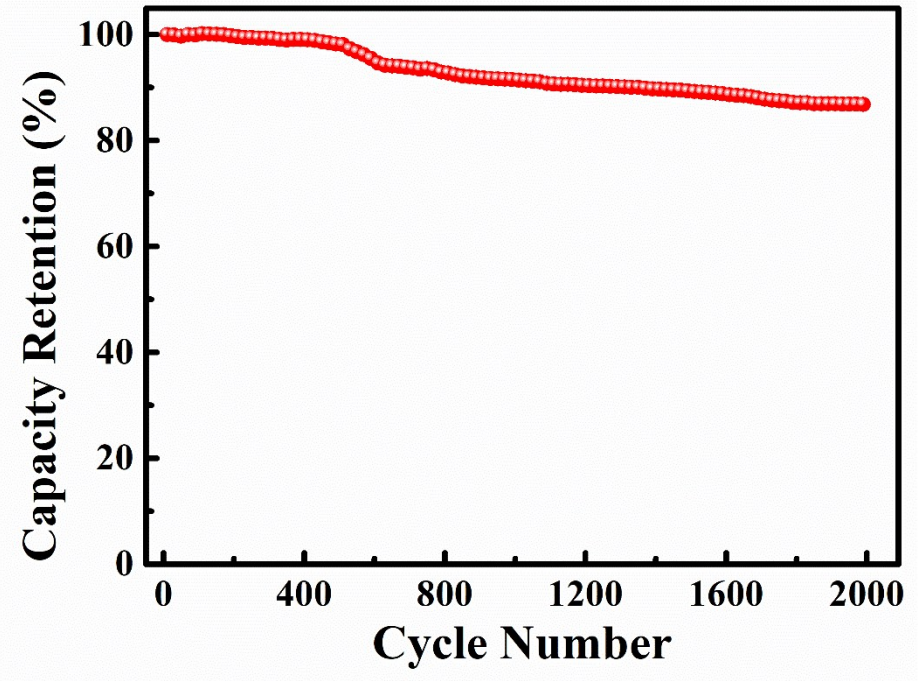

Figure S8 The capacity retention with the function of cycling number at 5 mA/cm^2.

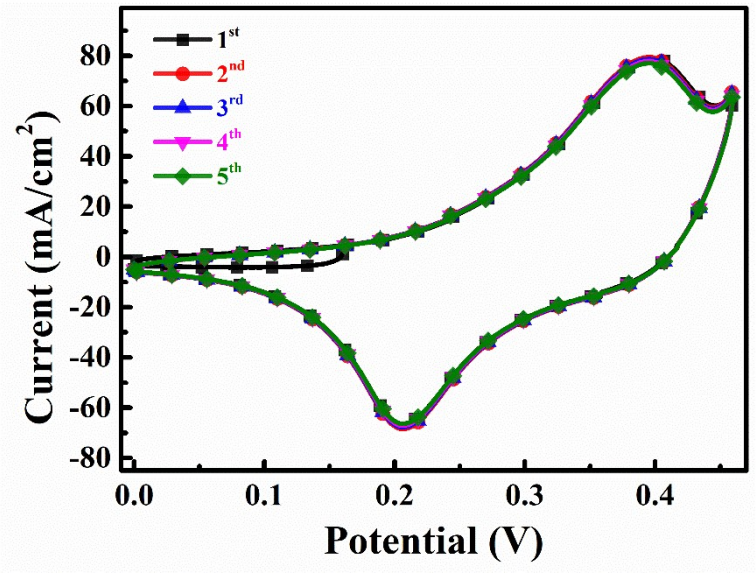

Figure S9 CV curves of Ni-MOF/CNTF initial five cycles at 10 mV/s.

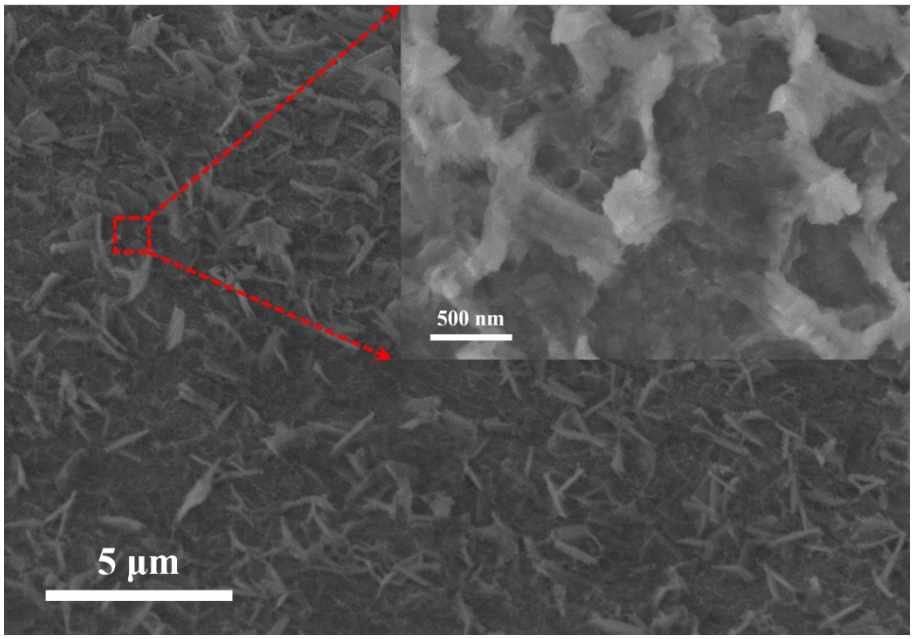

Figure S10 The SEM image of the Ni-MOF/CNTF sample after the circulation.

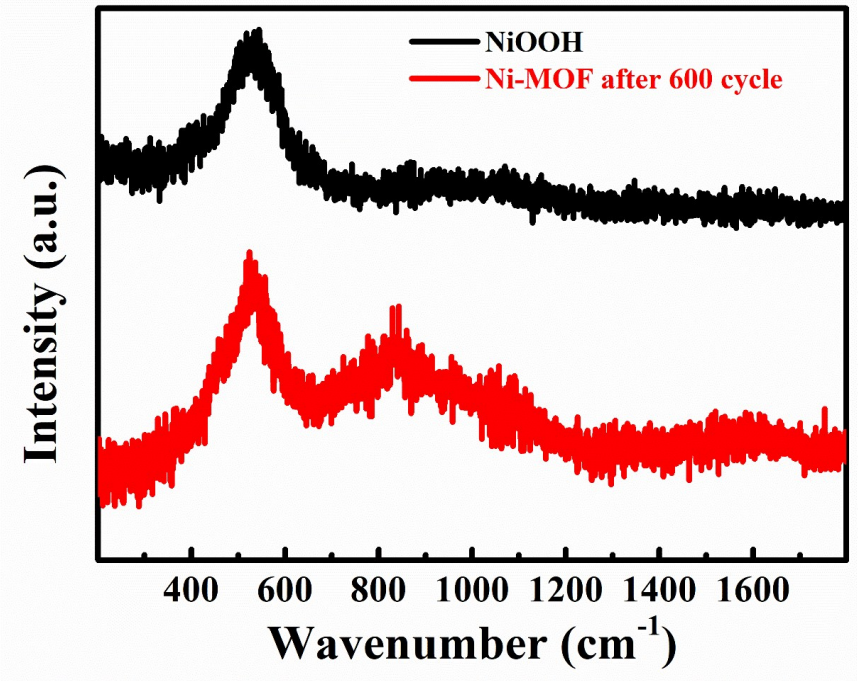

Figure S11 The Raman spectrum of the Ni-MOF sample after the circulation and NiOOH.

Figure S12 The schematic illustration of the FAR Ni-Zn battery.

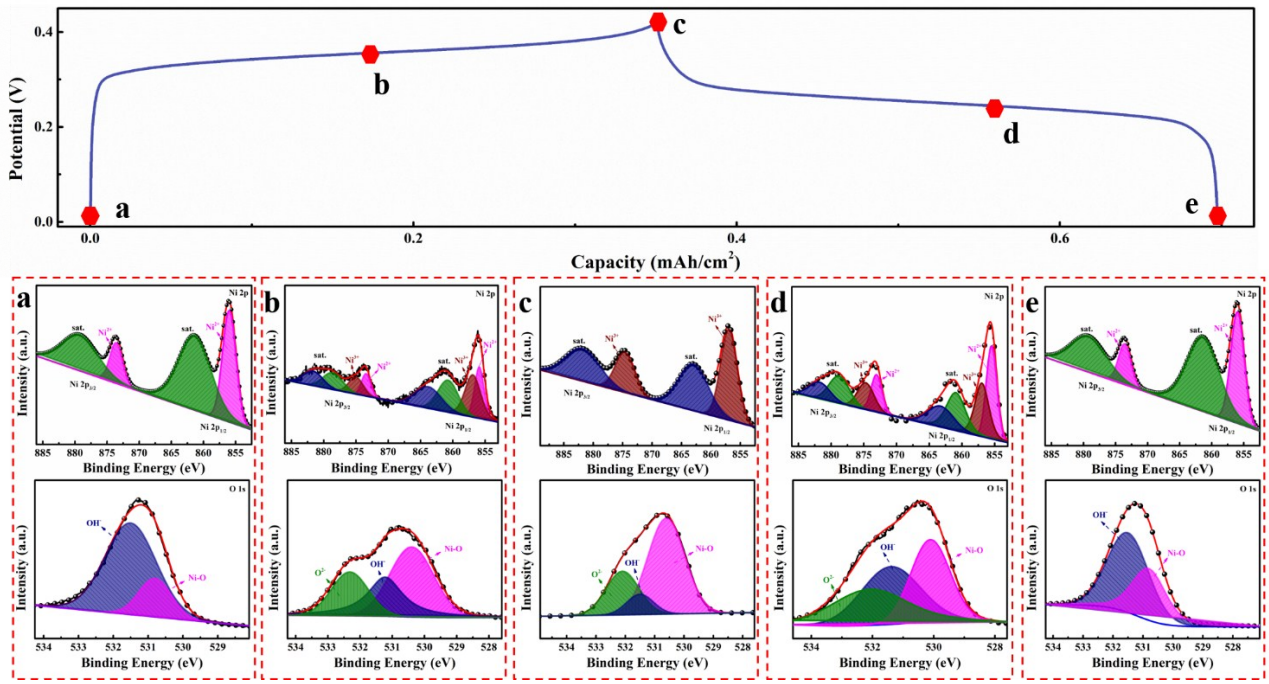

Figure S13 The ex-situ XPS spectrum of Ni-MOF/CNTF with the galvanostatic charge/discharge curve (current density of 5mA/cm^2) with a voltage range from 0 to 0.42 V.

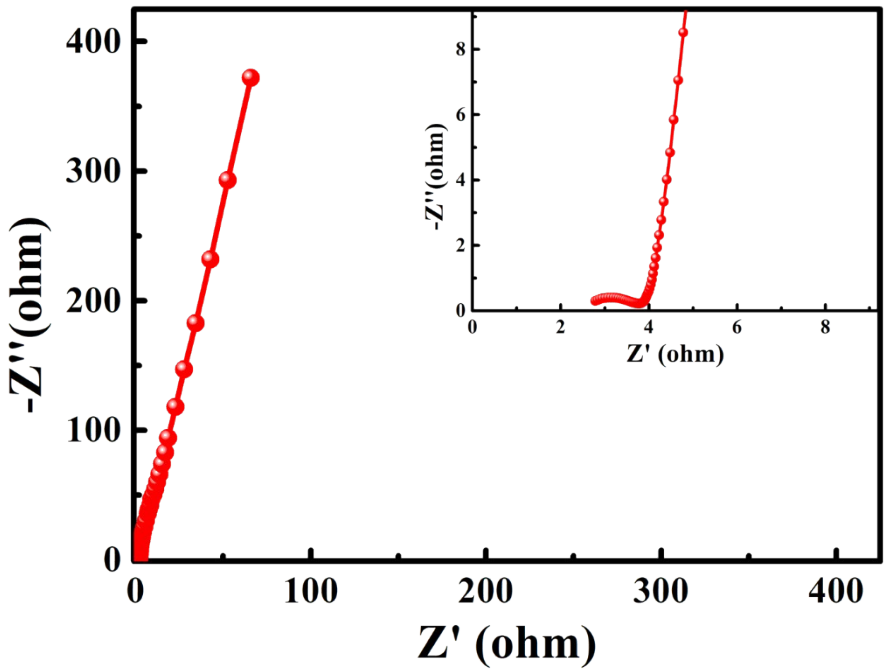

Figure S14 The Nyquist of the FAR Ni-Zn battery.

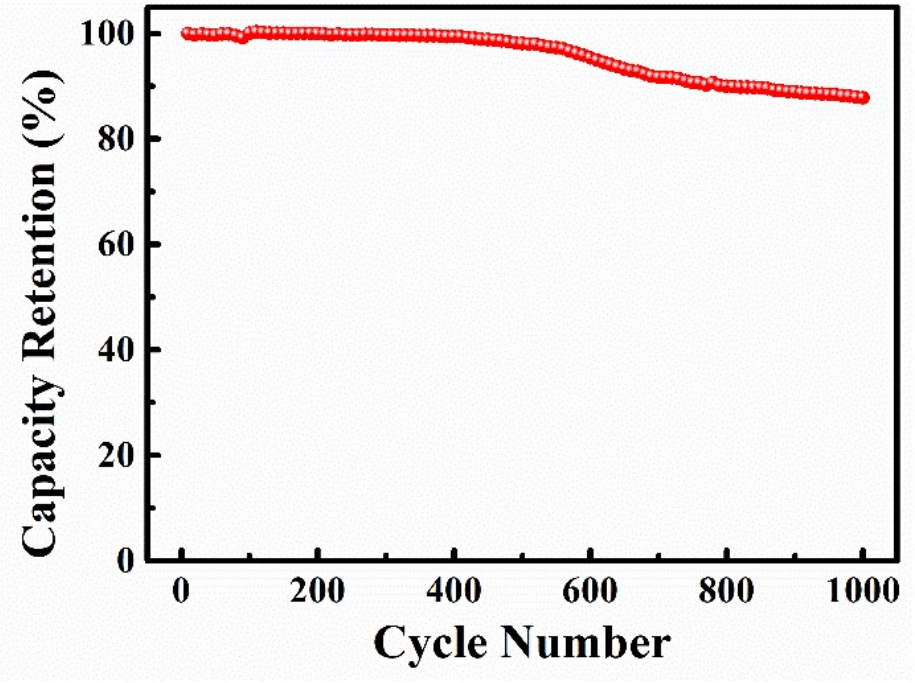

Figure S15 Cycle performance of the device at a current density of 0.5 mA/cm^2

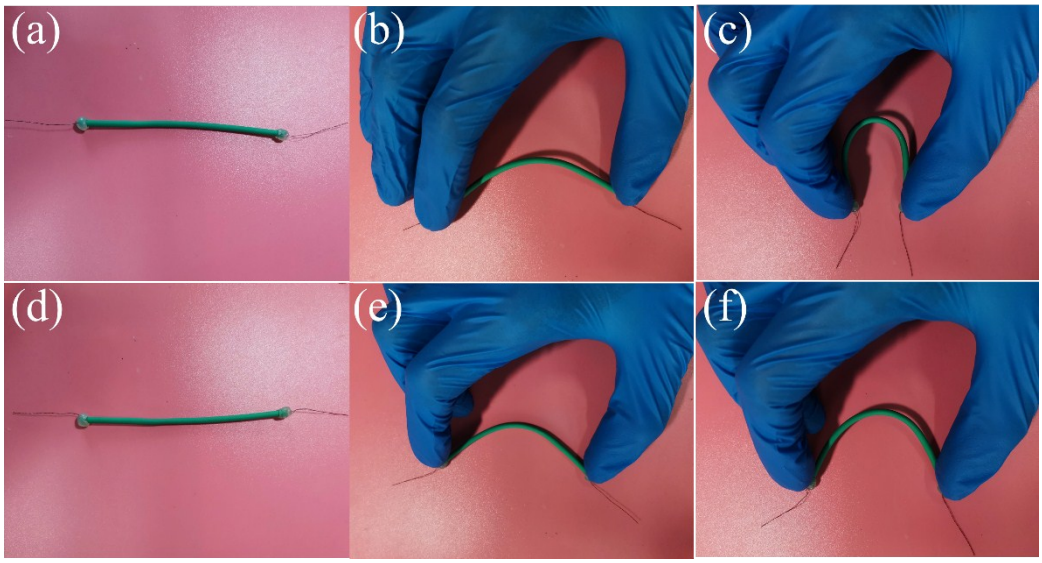

Figure S16 The photo images of as-made FAR Ni-Zn battery at different bent angle.

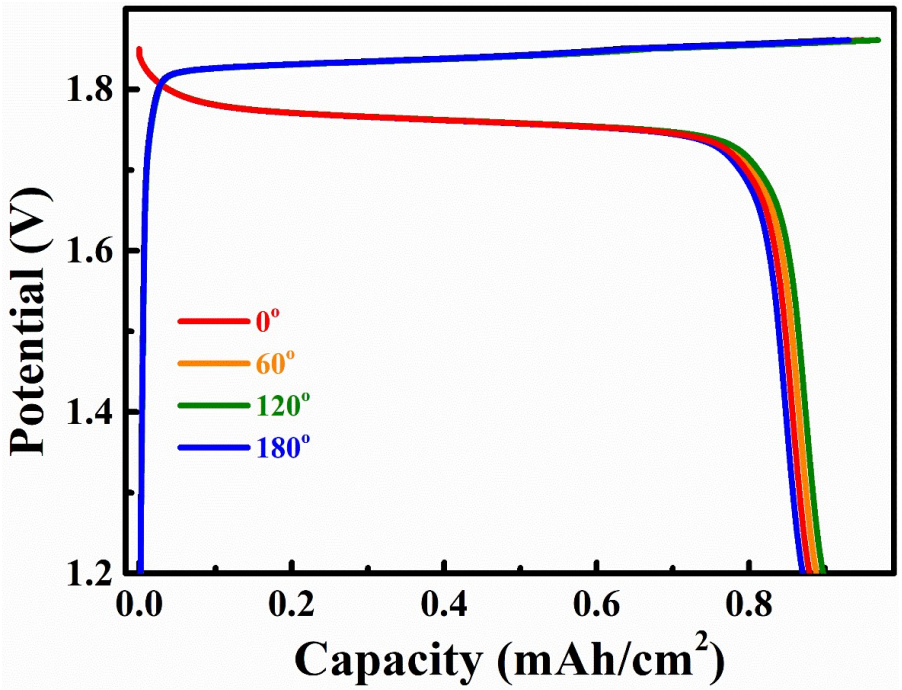

Figure S17 The GCD curves of the FAR Ni-Zn battery at different bent angles.

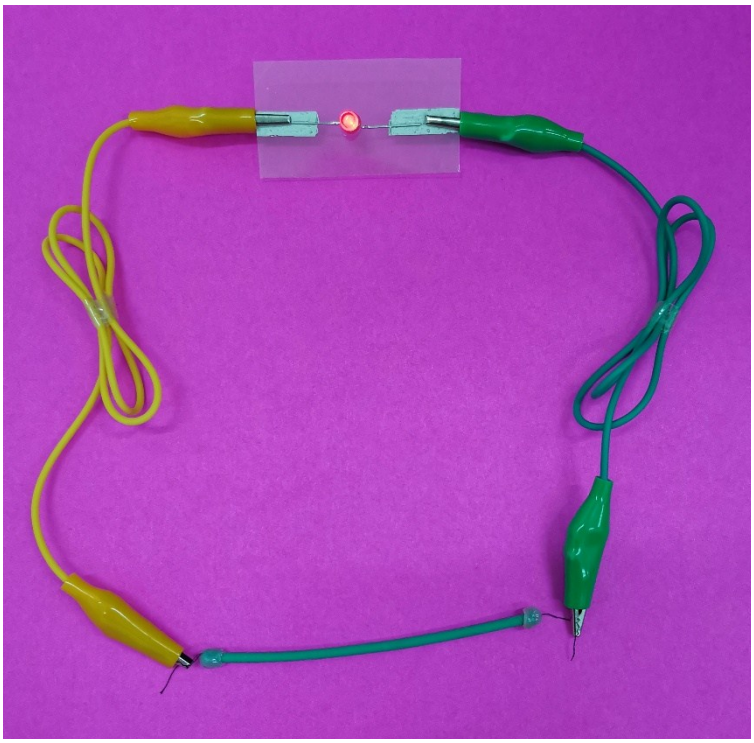

Figure S18 The photo images of a red LED powered by a single FAR Ni-Zn battery.

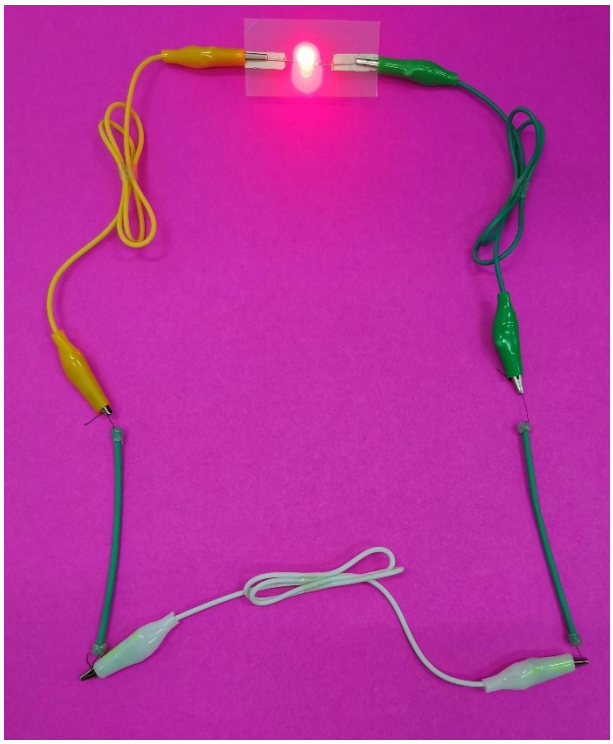

Figure S19 The images of a red LED powered by two as-made FAR Ni-Zn batteries in series.